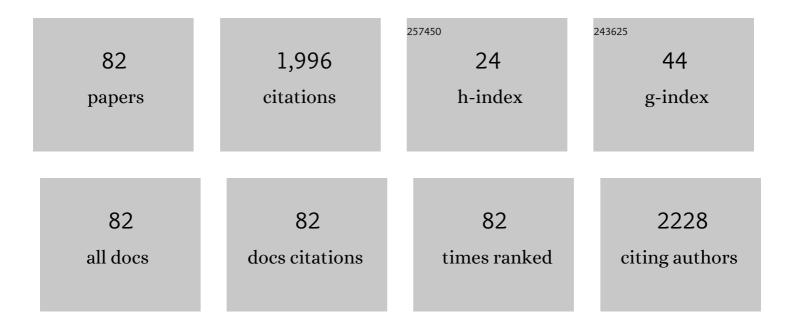
Toshio Kikuta

List of Publications by Year in descending order

Source: https://exaly.com/author-pdf/4796043/publications.pdf Version: 2024-02-01



Τοςμίο Κικιιτλ

#	Article	IF	CITATIONS
1	Microstructure and H2 gas sensing properties of undoped and Pd-doped SnO2 nanowires. Sensors and Actuators B: Chemical, 2009, 135, 524-529.	7.8	188
2	O2 and CO sensing of Ga2O3 multiple nanowire gas sensors. Sensors and Actuators B: Chemical, 2008, 129, 666-670.	7.8	169
3	Influence of effective surface area on gas sensing properties of WO3 sputtered thin films. Thin Solid Films, 2009, 517, 2069-2072.	1.8	149
4	Room temperature gas sensing of p-type TeO2 nanowires. Applied Physics Letters, 2007, 90, 173119.	3.3	103
5	Preparation of WO3 nanoparticles and application to NO2 sensor. Applied Surface Science, 2009, 256, 1050-1053.	6.1	103
6	Hydrogen sensors made of undoped and Pt-doped SnO2 nanowires. Journal of Alloys and Compounds, 2009, 488, L21-L25.	5.5	97
7	Influence of morphology and structure geometry on NO2 gas-sensing characteristics of SnO2 nanostructures synthesized via a thermal evaporation method. Sensors and Actuators B: Chemical, 2011, 153, 11-16.	7.8	96
8	Influence of annealing on microstructure and NO2-sensing properties of sputtered WO3 thin films. Sensors and Actuators B: Chemical, 2007, 128, 173-178.	7.8	90
9	Catalyst supported growth of In2O3 nanostructures and their hydrogen gas sensing properties. Sensors and Actuators B: Chemical, 2010, 147, 48-54.	7.8	86
10	Preparation of tungsten oxide nanowires and their application to NO2 sensing. Sensors and Actuators B: Chemical, 2012, 169, 113-120.	7.8	65
11	Preparation and gas sensing properties of undoped and Pd-doped TiO2 nanowires. Sensors and Actuators B: Chemical, 2014, 190, 838-843.	7.8	60
12	H2S sensing property of porous SnO2 sputtered films coated with various doping films. Vacuum, 2006, 80, 723-725.	3.5	55
13	Fabrication and gas sensing properties of In2O3 nanopushpins. Applied Physics Letters, 2009, 95, .	3.3	50
14	Porous SnO2 sputtered films with high H2 sensitivity at low operation temperature. Thin Solid Films, 2008, 516, 5111-5117.	1.8	49
15	Dependence of NO2 gas sensitivity of WO3 sputtered films on film density. Thin Solid Films, 2005, 474, 255-260.	1.8	42
16	A generic approach for controlled synthesis of In2O3 nanostructures for gas sensing applications. Journal of Alloys and Compounds, 2009, 481, L35-L39.	5.5	42
17	Synthesis and Characterization of TeO ₂ Nanowires. Japanese Journal of Applied Physics, 2008, 47, 771.	1.5	41
18	Synthesis of metal and metal oxide nanostructures and their application for gas sensing. Materials Chemistry and Physics, 2011, 127, 143-150.	4.0	39

#	Article	IF	CITATIONS
19	Effect of density and thickness on H2-gas sensing property of sputtered SnO2 films. Vacuum, 2005, 77, 237-243.	3.5	36
20	Hydrogen sensing properties of Pd-doped SnO2 sputtered films with columnar nanostructures. Thin Solid Films, 2009, 517, 6119-6123.	1.8	36
21	Effect of micro-electrode geometry on NO2 gas-sensing characteristics of one-dimensional tin dioxide nanostructure microsensors. Sensors and Actuators B: Chemical, 2011, 156, 784-790.	7.8	36
22	Dealloying Derived Synthesis of W Nanopetal Films and Their Transformation into WO ₃ . Journal of Physical Chemistry C, 2008, 112, 1391-1395.	3.1	35
23	NO2 response enhancement and anomalous behavior of n-type SnO2 nanowires functionalized by Pd nanodots. Sensors and Actuators B: Chemical, 2012, 166-167, 671-677.	7.8	34
24	Catalyst-free shape controlled synthesis of In2O3 pyramids and octahedron: Structural properties and growth mechanism. Journal of Alloys and Compounds, 2009, 480, L9-L12.	5.5	24
25	Ferroelectric Properties of Deuterated Glycine Phosphite. Ferroelectrics, 2002, 269, 153-158.	0.6	20
26	Influence of an Electric Field Perpendicular to the Ferroelectric Axis on the Dielectric Properties of Triglycine Sulfate. Ferroelectrics, 2006, 336, 91-100.	0.6	18
27	Lining of hydraulic cylinder made of cast iron with copper alloy. Journal of Materials Processing Technology, 2006, 172, 30-34.	6.3	15
28	Effective Surface Area of SnO2-Sputtered Films Evaluated by Measurement of Physical Adsorption Isotherms. Japanese Journal of Applied Physics, 2006, 45, 9180-9184.	1.5	15
29	Synthesis of Titanate Nanorods by High-Temperature Oxidation. Journal of Physical Chemistry C, 2008, 112, 4545-4549.	3.1	14
30	Crystal Structure of the Ferroelectric Phase of Triglycine Sulfate under an Electric Field. Ferroelectrics, 2007, 347, 65-73.	0.6	13
31	NO2Gas Sensor Made of Porous MoO3Sputtered Films. Japanese Journal of Applied Physics, 2005, 44, 792-795.	1.5	12
32	Domain Pattern of Triglycine Sulfate after Exposure to an Electric Field Perpendicular to the Ferroelectric Axis. Journal of the Korean Physical Society, 2007, 51, 754.	0.7	12
33	Ferroelectric Phase Transition Character of Glycine Phosphite. Ferroelectrics, 2006, 332, 13-19.	0.6	10
34	Dielectric properties and phase transition in cesium tetrachlorozincate Cs2ZnCl4. Ferroelectrics, 1992, 125, 141-146.	0.6	9
35	Preparation of Ferroelectric Glycine Phosphite Single Crystals. Japanese Journal of Applied Physics, 2000, 39, 6612-6613.	1.5	9
36	Growth and internal bias field of l-lysine-doped triglycine sulfate (LLysTGS). Journal of Crystal Growth, 2007, 307, 372-377.	1.5	9

#	Article	IF	CITATIONS
37	Dilatometric Study on Monoclinic Crystals of Ferroelectric TGS Down to Cryogenic Temperature Region. Ferroelectrics, 2006, 337, 59-69.	0.6	8
38	Fabrication of WO3 Nanoflakes by a Dealloying-based Approach. Chemistry Letters, 2008, 37, 296-297.	1.3	8
39	Growth and ferroelectric properties of l-, d-, and dl-methionine-doped triglycine sulfate crystals. Journal of Crystal Growth, 2010, 313, 20-25.	1.5	8
40	Microstructure and Gas Sensing Property of Porous SnO ₂ Sputtered Films. Materials Science Forum, 2007, 539-543, 3508-3513.	0.3	6
41	Order-Disorder Structure of Triglycine Sulfate Under Electric Field. Ferroelectrics, 2010, 403, 111-118.	0.6	6
42	Preferences of polarity and chirality in triglycine sulfate crystals by alanine ghost. Journal of Physics and Chemistry of Solids, 2021, 151, 109890.	4.0	6
43	A calorimetric study of RS1-xARSx mixed crystal system (0.9 ≲ x < 1.0). Ferroelectrics, 1995, 168, 169-175.	0.6	5
44	Domain structure in the polar phase of ammonium rochelle salt. Ferroelectrics, 1997, 190, 51-56.	0.6	5
45	Phase transition of copper-doped triglycine sulfate. Ferroelectrics, 2001, 262, 119-124.	0.6	5
46	Deuteration Effect on the Ferroelectric Phase Transition of TAAP. Ferroelectrics, 2006, 337, 95-103.	0.6	5
47	Dielectric Dispersion of Triglycine Sulfate at Ferroelectric Phase. Ferroelectrics, 2002, 272, 351-356.	0.6	4
48	Growth and Domain Structure of TGS Crystals Doped with Various Amino Acids. Ferroelectrics, 2008, 368, 12-22.	0.6	4
49	Dielectric Character Modified by Perpendicular Electric Field in Triglycine Sulfate. Ferroelectrics, 2008, 367, 163-169.	0.6	4
50	Transverse field effect close to the critical point in the TGS ferroelectric. Philosophical Magazine, 2011, 91, 3755-3765.	1.6	4
51	Influence of side electric potential on hysteresis loop parameters and electric permittivity in the Rochelle salt. Physica B: Condensed Matter, 2012, 407, 3956-3959.	2.7	4
52	Pyroelectric properties of the triglycine sulphate crystal formerly influenced by a transverse electric field. Philosophical Magazine, 2015, 95, 289-300.	1.6	4
53	Polarization reversal of telluric acid ammonium phosphate. Materials Science and Engineering B: Solid-State Materials for Advanced Technology, 2005, 120, 134-136.	3.5	3
54	Influence of Various Amino Acids Doping on Growth and Domain Structure of Tgs Crystals. Ferroelectrics, 2010, 403, 38-44.	0.6	3

#	Article	IF	CITATIONS
55	Influence of Prolonged Application of Transverse Electric Field on Remanent Polarization in Rochelle Salt. Ferroelectrics, 2012, 430, 20-29.	0.6	3
56	Molecular motion of PO ₄ in KDP at ferroelectric phase transition. Ferroelectrics, 1995, 170, 17-22.	0.6	2
57	Slit Structure as a Countermeasure for the Thermal Deformation of a Metal Mask. Japanese Journal of Applied Physics, 2001, 40, 7170-7173.	1.5	2
58	Temperature Dependence of Dielectric Dispersion in TGS Influenced by Perpendicular Electric Field. Ferroelectrics, 2009, 384, 113-119.	0.6	2
59	Thickness Distribution of Metal Films by Magnetron Sputtering. Journal of the Vacuum Society of Japan, 2011, 54, 184-187.	0.3	2
60	A transverse electric current in triglycine sulphate ferroelectric crystal. Philosophical Magazine, 2016, 96, 1332-1343.	1.6	2
61	Structural change in the paraelectric phase of ammonium Rochelle salt. Ferroelectrics, 1999, 229, 189-194.	0.6	1
62	X-Ray diffraction intensity of ammonium rochelle salt having domain structure. Ferroelectrics, 1999, 222, 243-247.	0.6	1
63	Dielectric Dispersion in the Middle of Polarization Reversal in Triglycine Sulfate Crystals. Ferroelectrics, 2003, 290, 187-192.	0.6	1
64	Influence of Uniaxial Pressure on the Phase Transition of Partially Deuterated Glycinium Phosphite. Ferroelectrics, 2004, 302, 99-104.	0.6	1
65	Dielectric Dispersion around the Ferroelectric Phase Transition in Partially Deuterated Glycine Phosphite. Ferroelectrics, 2007, 355, 204-210.	0.6	1
66	Application of TiAl laminate to a sputtering target for TiAlN films. Vacuum, 2008, 83, 479-482.	3.5	1
67	Porosity Assessment of NiO Sputtered Film and NO2 Sensing Property. Journal of the Vacuum Society of Japan, 2010, 53, 226-229.	0.3	1
68	Nanostructure of WO3 Sputtered Films Deposited at Various Gas Pressures. Journal of the Vacuum Society of Japan, 2010, 53, 210-213.	0.3	1
69	Degree of Order by X-Ray Crystal Structure Analysis in Triglycine Sulfate. Ferroelectrics, 2012, 427, 119-128.	0.6	1
70	Polarization Reversal in TGS after Application of Transverse Electric Field. Ferroelectrics, 2013, 443, 88-94.	0.6	1
71	Superlattice structure of ars in the polar phase. Ferroelectrics, 2001, 261, 245-250.	0.6	0
72	Simple Model using Gas Sensor Characteristics of each Component Gas to Estimate Individual Gas Concentrations in Gas Mixtures. Japanese Journal of Applied Physics, 2003, 42, 1538-1544.	1.5	0

#	Article	IF	CITATIONS
73	Exact Determination of the Polar Direction in Lithium Trihydrogen Selenite Ferroelectric Crystal. Japanese Journal of Applied Physics, 2003, 42, 6483-6485.	1.5	0
74	Lining of Cast Iron Cylinder with Copper Alloy. Advanced Materials Research, 2006, 15-17, 888-893.	0.3	0
75	Strange Thermal Expansion of Ferroelectric TGS in the Cryogenic Temperature Region. Ferroelectrics, 2008, 368, 28-35.	0.6	0
76	Annealing Effect on the Nanostructure of TiO2 Sputtered Film and H2 Sensing Property. Journal of the Vacuum Society of Japan, 2010, 53, 353-356.	0.3	0
77	Lining of cast iron cylinder with copper alloy utilising high temperature oxidation. International Journal of Cast Metals Research, 2011, 24, 124-126.	1.0	Ο
78	Calorimetric Study of Triglycine Sulfate after Prolonged Application of Transverse Electric Field. Ferroelectrics, 2012, 430, 30-35.	0.6	0
79	Thickness Distribution of Metal Films by Magnetron Sputtering (II) ^ ^mdash;Effect of the Distance between the Target and Substrate and the Erosion Distribution^ ^mdash;. Journal of the Vacuum Society of Japan, 2013, 56, 382-385.	0.3	Ο
80	Influence of Transverse Electric Field on Dielectric Permittivity of Triglycine Sulfate. Ferroelectrics, 2014, 462, 39-46.	0.6	0
81	Role of Bias Electric Field for X-ray Diffraction Intensity by TGS Crystal in Transverse Electric Field. Ferroelectrics, 2015, 485, 27-33.	0.6	0
82	TGS crystal as a maximum temperature thermometer. Philosophical Magazine, 2021, 101, 491-500.	1.6	0